STRESS WAVES IN SOILS IN THE PRESENCE OF CAVITATION EFFECTS

V. A. Kotlyarevskii, E. G. Maiorova, and A. I. Shishikin

UDC 532.593

Internal fractures in different materials, associated with stress waves caused by short-lived pulses [1] reflected from free boundaries, complicate the solution of wave problems. The possibility of crack formation (cavitation) under impact on an elastoplastic rod is shown in [2], while the procedure for a correction in the computation of axisymmetric elastoplastic flows of a medium under the explosive action associated with the crack-formation process, by a mesh method is described in general terms in [3]. A formulation and numerical solution of the one-dimensional problem of pulse loading of a soil layer in a gravity force field is presented in this paper. The model of the soil is taken by a somewhat modified rheological Denisov–Murayami scheme corresponding to the properties of clayey soil under volume strain [4]. It is assumed that the medium possesses the rupture strength limit, which specifies the origination and snapping of cracks under definite conditions. A comparison between computations and an experiment conducted on a coarsely dispersed viscoelastic material is presented.

§1. The one-dimensional problem of a vertical column supported on a rigid obstacle (the load is applied to the free surface or is produced by motion of the obstacle) is considered. In connection with the possibility of the appearance of shock and cavitation fronts in the medium, it is usually required to formulate conditions on these moving boundaries. A finite-element approximation of the equations of the process and the method of a through computation with artificial viscosity of the Neumann–Richtmyer type [5], which automatically assures taking account of ruptures in continuity as well as shock transitions (somewhat spread out), are used. The cavitation effects are checked by using logic operators in the algorithm of the problem.

The model of continuous sections of the medium for axial compression conditions (Fig. 1) is constructed from elements of elastic H_j ($p^0 = C_j\xi$), viscous N_j ($p^0 = \mu_j\dot{\xi}$), and Coulomb friction K ($p^0 = \sigma_+ \operatorname{sgn}\dot{\xi}$ for $\xi \neq 0$ and $\dot{\xi} = 0$ for $|p^0| < \sigma_+$), which specifies partial irreversibility of the strain. Here p^0, ξ are the pressure and relative compressive strain of an individual element, C_j is the elastic modulus, μ_j is the coefficient of viscosity ($j = 1, 2$), σ_+ is the yield point, $(\ )^{\cdot} \equiv \partial(\ )/\partial t$, and t is the time. It is considered that $\mu_1 \ll \mu_2$, where μ_1 corresponds to the artificial viscosity in order of magnitude. Therefore, the elastic behavior under loading is bounded by the quantity σ_+, outside of whose limits viscoelastoplastic properties appear. At comparatively high pressures p (when $p \gg \sigma_+$) the influence of σ_+ is small and the viscoelastic behavior of the model corresponds to a generalized Voigt model with two lag times. In order to reproduce the experimental values of the residual strain in this case, it is sufficient to give an elevated value (during unloading) to the parameter σ_+ [i.e., one of two values is given to σ_+ during solution of the problem: $\sigma_+^{(1)}$ for loading and $\sigma_+^{(2)}$ for unloading].

The model has the structural formula $(H_1 | N_1) - (H_2 | N_2 | K)$, in which the vertical bar denotes a parallel and the horizontal bar a series connection of the elements. The presence of dissipative elements results in a set of pressure–strain ($p \sim \varepsilon$) diagrams whose shape depends on the strain mode. For very high velocities and small μ_1 (on the order of the artificial viscosity), the upper envelope of the diagrams will correspond to the

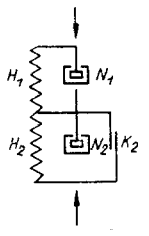

Fig. 1

Moscow. Translated from Zhurnal Prikladnoi Mekhaniki i Tekhnicheskli Fiziki, No. 2, pp. 95-104, March-April, 1978. Original article submitted February 21, 1977.

0021-8944/78/1902-0218$07.50

diagram of a loop with $j = 1(H_1 | N_1)$, which depends weakly on the strain rate. For slow (quasistatic) strain of the medium, its properties are expressed by the structural formula $(H_1 - (H_2 | K))$. Less complex rheological bodies – Maxwell, Voigt, Prandtl, Shvedov–Bingham, a standard linear body used earlier to identify the behavior of different soils [4] – are generalized by the model of Fig. 1.

The strain law for the model in Fig. 1 has the form $(\mu_1 + \mu_2 \neq 0)$

$$p = C_1\varepsilon_1 + \mu_1\dot{\varepsilon}_1; \tag{1.1}$$

$$\dot{\varepsilon}_1 = \dot{\varepsilon} \quad (|R| < \sigma_+, \quad R \equiv C_1\varepsilon_1 + \mu_1\dot{\varepsilon}_1 - C_2\varepsilon_2); \tag{1.2}$$

$$(\mu_1 + \mu_2)\dot{\varepsilon}_1 + (C_1 + C_2)\varepsilon_1 = \mu_2\dot{\varepsilon} + C_2\varepsilon + \sigma_+ \operatorname{sgn}\dot{\varepsilon}_2 (\dot{\varepsilon}_2 \equiv \dot{\varepsilon} - \dot{\varepsilon}_1 \neq 0); \tag{1.3}$$

$$\sigma_+ = \begin{cases} \sigma_+^{(1)} & (R > 0), \\ \sigma_+^{(2)} & (R < 0), \end{cases} \tag{1.4}$$

where R is the pressure in an element K for $\dot{\varepsilon}_2 \equiv 0$ (i.e., without slip), $\varepsilon_1\varepsilon_2$ are the strains of the upper and lower stories (links) of the model, respectively, and $\varepsilon = \varepsilon_1 + \varepsilon_2$ is the total relative strain. Under the primary loading $\varepsilon_2 = 0$ and the behavior of the medium is determined by the relationships (1.1) and (1.2). From the time the condition $t = t^*$ is spoiled for (1.2), Eq. (1.3) is integrated, where the continuity of ε_1 and the transient condition $\operatorname{sgn}\dot{\varepsilon}_2(+t^*) = \operatorname{sgn}R(-t^*)$ are taken into account. Then, if the condition for (1.3) is spoiled during unloading, the friction in K checked by a change in the sign of the velocity $\dot{\varepsilon}_2$ ceases and a return to (1.2) is realized, where the strain ε_2 remains constant, since $\dot{\varepsilon}_2 = 0$, etc. The relationship (1.4) develops the value of σ_+ in (1.3) and in the condition for (1.2) for arbitrary modes of the change in p(t) [the initial value is $\sigma_+ = \sigma_+^{(1)}$]. It is later assumed that the initial strain of the medium, compressed by the actual pressure, is due to the stiffness of the element H_1, while an elastic element H_2 is unloaded completely because of secondary relaxation mechanisms. This condition of initial static equilibrium corresponds to the excess of the value $\sigma_+^{(1)}$ over the actual pressures along the whole soil column, which results in gradients in the parameter σ_+ in the medium. As trial computations showed, this model reproduces wave processes in soft soils for pressures approximately up to 10^6 N/m^2.

The Lagrange coordinate x directed along the free-fall acceleration vector g with origin x = 0 superposed on the free surface (imaginary decompressed reduction of the actual pressures) of soil with density ρ_0. The actual pressure $p(x) = g\int_0^x \rho_0 dx$ causes the strain $\varepsilon = p/C_1$ and displacement of the particles in the layer

$$u(x, 0) = -\int_{l_*}^{x} \varepsilon(y)\, dy = -g\int_{l_*}^{x} C_1^{-1}(z)\int_0^z \rho_0(y)\, dydz,$$

where l_0 is the height of the layer in the decompressed state. Let us consider the mean density ρ and height l of the compressed layer given; then $l_0 = l + u(0, 0)$, $\rho_0 = \rho l l_0^{-1}$. For $\rho_0 = \text{const}$, $C_1 = \text{const}$, $u(0, 0) = {}^1/_2\rho_0 g l_0^2 C_1^{-1}$, $l_0 = l(1 - {}^1/_2 g\rho l/C_1)^{-1}$, $\rho_0 = \rho(1 - {}^1/_2 g\rho l/C_1)$.

The equations of motion and continuity of sections of a continuous medium have the form $(( )' \equiv \partial( )/\partial x)$

$$\rho_0\ddot{u} = -p' + g\rho_0; \tag{1.5}$$

$$\varepsilon = -u'. \tag{1.6}$$

The system of equations (1.1)-(1.6) is closed and describes the behavior of the continuous sections of the medium between the cracks. The initial conditions are determined by the displacements u(x, 0) and the zero velocities $\dot{u}(x, 0) = 0$. The boundary conditions have the form $p = H(t - t_1)f_1(t - t_1)$ for x = 0 and $\dot{u} = H(t)f_2(t)$ for $x = l_0$, where H(t) is the Heaviside function and t_1 is the phase shift of the boundary functions.

For the numerical solution, the conservation equations written down are referred to the finite element of the medium, which transfers the boundary-value problem into a Cauchy problem for the system of ordinary differential equations. Splitting the medium into an element with mass $\rho_0 h$ per unit area is done by means of the planes $x_i = hi$ (i = 0, 1, 2, . . . , n); i = 0 corresponds to the free surface and i = n to the obstacle. The spacing of the splitting $h = l_0/n$ is determined by the number of elements n. The system of conservation equations referred to a finite element of the medium (for centering the inertial properties at the points $x_{i\pm 1/2} = x_i \pm h/2$ and the strains at x_i) is equivalent to finite-difference equations if the derivatives with respect to the coordinate $( )'$ at the centering points are approximated in the form $p_i' = \nabla p_i h^{-1}$, $u_{i-1/2}' = \Delta u_{i-1/2} h^{-1}$ by using the difference operators $\nabla F_i = F(x_i) - F(x_i - h)$, $\Delta F_i = F(x_i + h) - F(x_i)$, and the time derivatives $( )^{\cdot}$ are assumed ordinary and all the functions are referred to the appropriate centering points.

Equations (1.5) and (1.6) are approximated in the form

$$\ddot{u}_{i-1/2} = -\nabla p_i(\rho_0 h)^{-1} + g; \tag{1.7}$$

$$\varepsilon_i = -\Delta u_{i-1/2} h^{-1}. \tag{1.8}$$

The deformation at the point i = n, bounding the solid wall, is determined by the relationship $\varepsilon_n = 2\left(u_n - \int_0^t H(z) f_2(z)\, dz\right) h^{-1}$, and at the point i = 0 by (1.1)-(1.4) for $p_0 = p(0, t)$. The initial conditions are also referred to the centering points.

The conditions for the origination of discontinuities in the continuum can be different depending on the physicomechanical properties of the medium. It is assumed below that the medium has a rupture strength σ and a zero resistance to rupture after collapse of the crack at the site of its formation, where the pressure in the crack equals zero (the possible gas flow into the crack from the boundary pressure is not taken into account).

The conditions for formation and closing of the crack are verified at the points i, i.e., at the joints of discrete elements with their continuous individual strain (creep) taken into account. The calculation procedure reduces to the following. The condition $p_i(t_i^0) \leq -|\sigma|$ is verified at each time spacing Δt of the numerical integration of the equations in all i. Its compliance corresponds to a primary rupture of the continuity in i at the time t_i^0, in which connection this value of i is stored. For $t > t_i^0$, for the mentioned value of i (taking account of the continuity of the displacements and the mass flow rates at the time of the transition t_i^0), the calculations of $u_{i\pm1/2}$ are continued by means of (1.7) for $p_i \equiv 0$ and those of the individual strains ε_i by means of (1.1)-(1.4) until dimensions δ_i^0 of the originating cracks exist:

$$\delta_i^0 = u_{i+1/2} - u_{i-1/2} + h\varepsilon_i \quad (t_i^0 < t < t_i^{00})$$

(for an element bounding the solid wall, h is taken with the coefficient 1/2). From the time t_i^{00} of closing of the crack ($\delta_i^0(t_i^{00}) = 0$), a return is made to the equations of the continuous medium. Subsequent ruptures are verified by the condition $p_i \leq 0$.

The mentioned checking procedure is carried out continuously, which permits taking account of the repeated appearance and collapse of the cracks. Therefore, if Eqs. (1.7), (1.2), or (1.3) are integrated for sections of the continuous medium, then (1.1) at $p_i = 0$ is integrated in addition for the discrete elements bounding the cracks, where (1.2) and (1.3) are used to calculate the individual strains ε_i.

§2. To verify the influence of the cell dimension h on the nature of the crack-formation reproducible in the computation, calculations were performed on the loading of a layer of a Voigt medium ($\rho_0 = 2.04 \cdot 10^3$ kg/m^3, $C_1 = 1.96 \cdot 10^7$ N/m^2, $\tau = \mu_1/C_1 = 0.5 \cdot 10^{-3}$ sec) with a zero resistance to rupture of height L = 2.5 m supported on a solid obstacle. The layer of medium is loaded by a pressure shock $p_0 = 2\rho_0 Lg$ during the time $\theta = L(C_1/\rho_0)^{-1/2}$. Since $\tau/\theta = 0.02 \ll 1$, the behavior of the medium should be almost elastic. The passage of an elastic wave to a solid obstacle corresponds to the pulse duration θ in a continuous elastic layer, and a tension exceeding the compression from its own weight first occurs at $t/\theta = 2.5$, $x/L = 0.5$, being propagated to the layer boundaries at the velocity of the elastic wave.

The change in the strain ε with time in different sections of the layer, obtained in the computations, is shown in Fig. 2 for $h_1 \equiv h(\rho_0 C_1)^{1/2}\mu_1 = 5$; 2 and 0.5 (curves 1-3, respectively). The time-counting spacing was taken from the condition $\Delta t = \mu_1 h_1 K/C_1$ in which the number K was determined from the expression $K = [(1.5h_1^2 + 1)^{1/2} - 1](2h_1)^{-1}$ [6] for $h < 2$ and $K = 0.5$ for $2 \leq h \leq 5$. The contribution of the viscous stresses in the high-strain-rate zones does not exceed 10%. The initial phase of the exact solution for an elastic layer compressed initially by its own weight is shown by the lines 4, where the beginning of the tension of the center of the layer is noted by the arrow. A change in the relative dimension $\delta = \delta^0/h$ of the cracks in the period when $p = O(\varepsilon \sim 0)$ is shown in the lower part of the graphs. Cavitation also originates in a Voigt medium at the center of the layer at the same time, where the upper part of the half-layer disperses almost instantaneously. The primary cavitation wave is propagated to the obstacle at the velocity $\sim 1.1(C_1/\rho_0)^{1/2}$, and the front of crack collapse moves from the bottom up at a considerably lower velocity. The degree of growth in the fluctuation amplitude with the dimension h of the finite element is seen from the graphs; however, for $h_1 \leq 2$ the reproduction of the functions ε, δ is sufficiently stable in the whole considered time interval containing two cavitation phases. The fluctuations ceased for $h_1 \leq 0.5$ and the solution became independent of the size of the element.

§3. Results are presented for a numerical computation of compression wave interaction with a solid located in the soil. The system of equations in Sec. 1 were supplemented by the equation of body motion

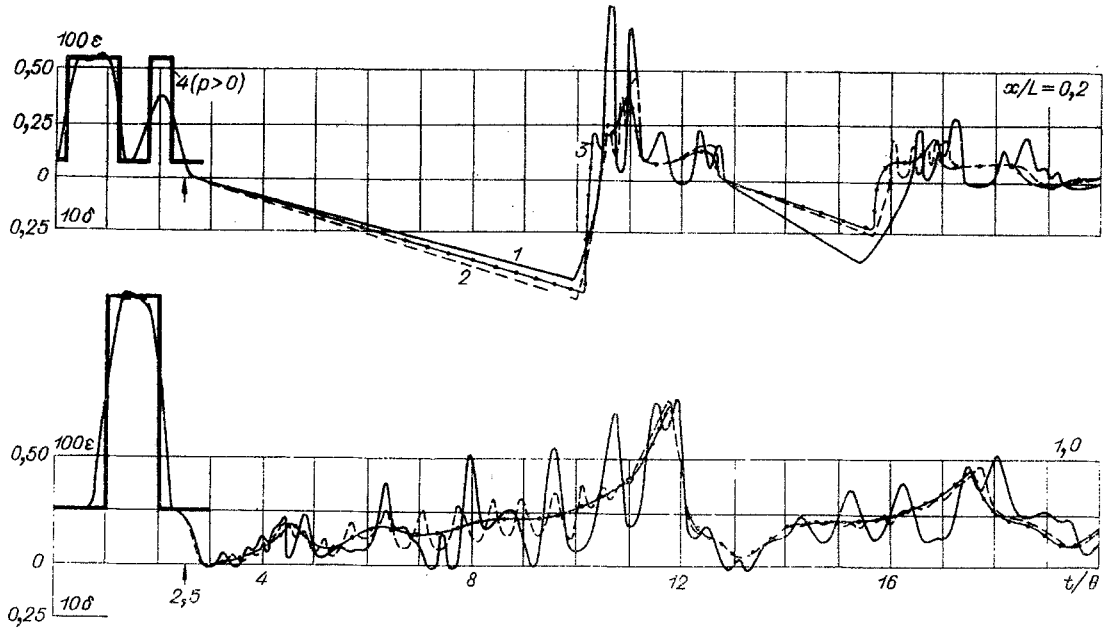

Fig. 2

$$d^2U/dt^2 = -[p(x_* + \chi, t) - p(x_*, t)]m^{-1} + g, \tag{3.1}$$

where U is the displacement of a body of thickness χ, x_* is the Lagrange coordinate of its upper face, and m is the specific mass of the body. Prior to the formation and after the collapse of the crack, (3.1) yields the boundary conditions to (1.5) at the two sections of the medium into which the layer is divided by the body: $u(x_*, t) = u(x_* + \chi, t)$, $u(x_*, t) = u(x_* - \chi, t)$. Therefore, (3.1) is included in the system of ordinary equations (1.7), and the quantity h is taken with the coefficient 1/2 in the calculation of the strain in the medium on the boundaries with the solid by means of (1.8).

The material constants of the model of the medium were selected experimentally (the soil is sand, the humidity by weight is 10-12%, and $\rho_0 = 1.47 \cdot 10^3$ kg/m^3). The equilibrium pliability I and time τ corresponding to the principal maximum of the lag spectrum were found in a first approximation from creep tests (under uniaxial strain of a thin soil layer due to the action of a step load $\sim 10^5$ N/m^2). The quantity C_1 was taken by means of the propagation velocity of weak perturbations in the soil and μ_1 by means of the condition for the artificial viscosity (see Sec. 2), i.e., $C_2 = C_1(C_1 I - 1)^{-1}$, $\mu_2 = \tau C_2$. The quantities C_2, σ_+ were refined in a second approximation by adjusting the computed compression wave configuration to an experiment conducted on a soil layer packed in a rectangular tray of 0.7 m width, 3 m length, and L = 1.7 m depth with stiff, smooth vertical walls lubricated by Vaseline and covered by a polymer film. A rigid body (parallelepiped) with the parameters $\chi = 27$ cm, $m = 2.84 \cdot 10^2$ kg/m^2 ($x_* = 38.5$) was arranged in the soil.

An air shock with pressure $p_m = 1.2 \cdot 10^5$ N/m^2 at the front and duration $\theta = 0.1$ sec was propagated along the long side of the tray to produce a pressure on the soil surface.

Oscillogram specimens of the boundary pressure 1, the pressure on the body surface 2, and at the bottom of the tray 3 are presented in Fig. 3a.

The following values of the constants were used in the computations: $C_1 = 3.64 \cdot 10^7$ N/m^2, $C_2 = 7.85 \cdot 10^6$ N/m^2, $\mu_1 = 1.28 \cdot 10^4$ N·sec/m^2, $\mu_2 = 2.25 \cdot 10^4$ N·sec/m^2. The yield point was taken to be linearly increasing with depth $\sigma_+^{(i)} = a^{(i)} + b^{(i)}x$ (i = 1, 2), where $\sigma_+^{(1)}$ easily exceeds the actual pressure $a^{(1)} = 2 \cdot 10^3$ N/m^2, $b^{(1)} = b^{(2)} = \rho_0 g = 1.44 \cdot 10^4$ N/m^3; the constant $a^{(2)}$, regulating the unloading and residual strain tempos, varied.

The boundary pressure is introduced into the computation by tables (according to oscillogram 1 in Fig. 3a). The size of the element of the medium is taken to be h = 5.5 cm.

Results of a computation of the time change in the pressure and the pressure–strain diagram on a body surface x/L = 0.226 and at the tray bottom x/L = 0.968 (corresponding to oscillograms 2 and 3, Fig. 3a) are presented in Fig. 3b. The pressures in two analogous tests are shown by the points 1 and 2, and a computation for $a^{(2)} = a^{(1)}$, $a^{(2)} = 10a^{(1)}$, $a^{(2)} = 25a^{(1)}$, respectively, by curves 3-5. A growth in the parameter $a^{(2)}$ does not influence the initial phase of the process and the amplitude of the pressure, but results in an essential increase in the residual strain.

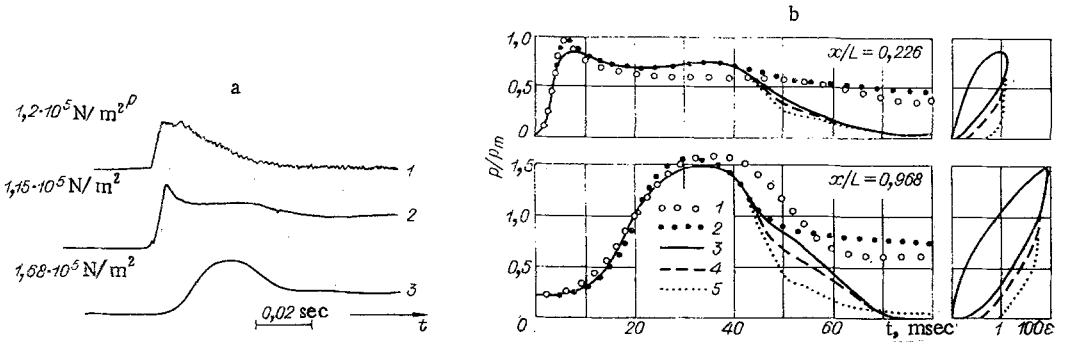

Fig. 3

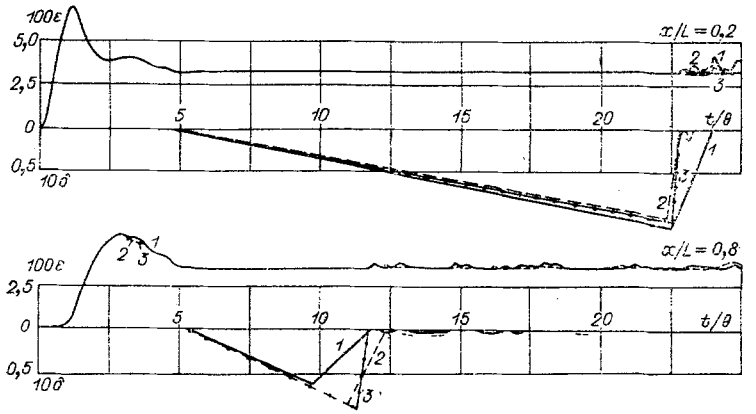

Fig. 4

Crack formation in a medium with soil parameters is possible under short pulses. A computation of compression wave passage into a homogeneous sand layer under the effect of a pressure shock $p_0 = 13.6\ \rho_0 Lg$ of duration $\theta = L(C_1/\rho_0)^{-1/2}$ is presented in Fig. 4 (it is assumed that $a^{(2)} = 2.45 \cdot 10^5\ N/m^2$). These computations are executed for the values $h_1 = 4.55$, 1.82, 0.455 (curves 1-3, respectively), where the identity of the reproduction and the unfolding of the cracks is seen. The difference in the times of crack collapse for h = 1.82 and 0.455 does not exceed 0.5θ in the range $t/\theta = 10$-24 and does not influence the residual strain distribution in the layer of the medium.

The use of the model in Fig. 1 is illustrated to describe wave processes in soft soils.

A. Propagation of Pressure Pulses Applied to the Free Layer Surface. The boundary pressure is taken in the form $p = p_m(1 - t/\theta)^{\alpha}$ in the computations. The values of the parameters are $p_m = 5 \cdot 10^5\ N/m^2$, θ = 0.25 sec, $\alpha = 4$. The time change in the pressure in the compression wave in a layer 25 m thick and at 0.5-5 m depths (in 0.5-m intervals) is shown by curves 1-10 in Fig. 5a.

The size of the element of the medium is taken at h = 25 cm in the computations and the artificial viscosity at $\mu_1 = 0.2 \cdot 10^5\ N \cdot sec/m^2$, $a^{(2)} \gg a^{(1)}$, while the remaining constants of the medium are the same as in Sec. 3 ($s \equiv t/\tau_2$ in Fig. 5).

The curve 0 corresponds to the boundary pressure. The computation is constrained by the (dimensionless) time s = 37, although the influence of the solid boundary is negligible, in which connection extinction of the pressure with depth and with time is observed.

The influence of a solid ($m = 4.43 \cdot 10^3\ kg/m^2$) located at a 3-m depth on the wave picture is shown in Fig. 5b. The pressure directly above the body is shown here by curve 6, while the pressure below it is shown by curve 7 and at every 0.5 m later by curves 8-11. The parameter $a^{(1)}$ is increased by the magnitude of the body weight in this computation for the soil under the body. The presence of a mass in the layer results in the origination of a reflected wave with the pressure $p/p_m = 1.05$.

B. Effect of a Seismic Perturbation on a Soil Layer Bounded by a Mass from Above. The seismic effect is modeled by displacement of the solid (lower) boundary of the layer according to the Berlag law:

$$u = a_0 \exp(-\varepsilon_0 t) \sin \omega t. \qquad (3.2)$$

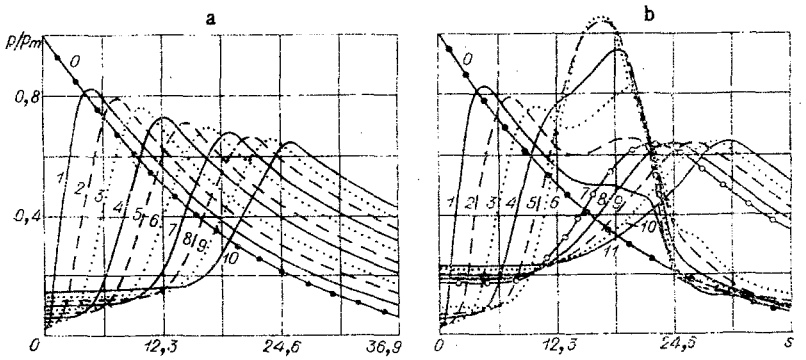

Fig. 5

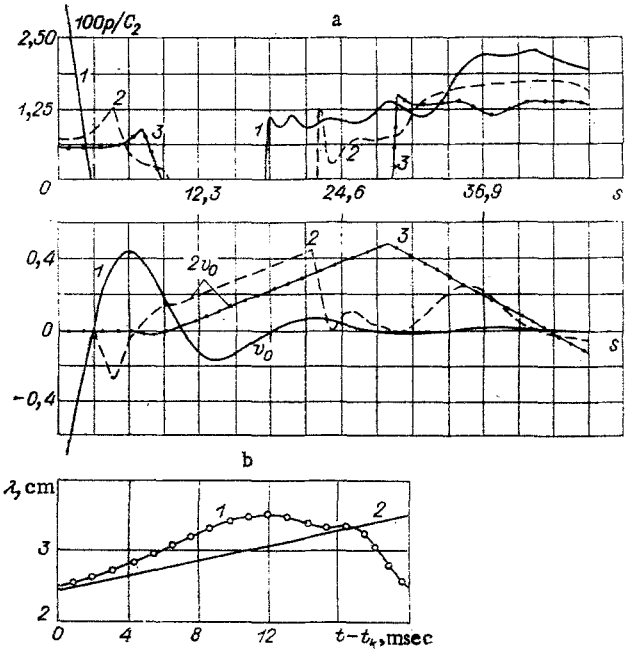

Fig. 6

The thickness of a soft soil layer is 2.5 m, $a_0 = 2$ cm, $\varepsilon_0 = 39.8$ sec^{-1}, $\omega = 125$ sec^{-1}, and the remaining parameters of the problem are the same as in the preceding computation. It is assumed that the medium has a zero resistance to rupture.

The change in pressure and the mass flow rates [$v_0 \equiv \dot{u}(\omega a_0)^{-1}$] in the layer with time is shown in Fig. 6a. The velocity corresponding to the boundary function (3.2) and the pressure under the layer are shown by the curves 1, the velocity and pressure at a 1-m depth by the curves 2, and the body velocity and the pressure under it by curves 3. Zones with zero pressure correspond to periods of crack opening. When an ejected body drops on the soil, the pressure under it reaches $p = 0.015\ C_2 = 2.7$ mg.

A comparison between computation and experiment of axial loading of a packet of thin cylindrical foam plates ($\rho_0 = 68.3$ kg/m^3) by an air shock is presented. The packet consisting of 10 cylinders of 5-cm diameter and 1.5 cm thickness each was mounted in a vertical position in a scaled Plexiglas chamber with a 5.2-cm-inner diameter and was drawn in by a rubber membrane from above. The pressure was applied through the membrane, where the packet was deformed under uniaxial stress state conditions. The shape of the pulse was approximated well by the expression $p = p_m(1 - t/\theta)^{\alpha}$, $p_m = 7.35 \cdot 10^5$ N/m^2, $\theta = 0.019$ sec, $\alpha = 3$.

The origination and opening of slots between cylinders in the packet were determined in tests by using high-speed moving pictures (3700 frames/sec), where the light source was mounted opposite the movie camera. A light strip on the moving picture film corresponded to the opening of the slot, where the bandwidth in connection with ligh diffraction exceeded the slot width. Hence, the spacings between centers of the light bands were measured in processing the experiments.

It was established by the tests that the packet disperses almost instantaneously from the time $t = t_k$, and deceleration of the dispersion associated with the resistance of the membrane starts for $t - t_k = 8$ msec. The

time change in the spacing $\lambda(t)$ between centers of two light bands, one of which was between the 6 and 7 and the other between the 8 and 9 cylinders (counting from the top), is shown by curve 1 in Fig. 6b.

Constants of the material in application to a two-element Voigt model were first obtained in creep tests for the computation: $C_1 = 7 \cdot 10^6$ N/m^2, $C_2 = 6 \cdot 10^5$ N/m^2, $\mu_1 = 1.5 \cdot 10^3$ N$\cdot$sec/m^2, $\mu_2 = 2 \cdot 10^3$ N$\cdot$sec/m^2. The results of the computation, performed on the effect of the above-mentioned nonstationary pulse (for $\sigma_+ = 0$, h = 1.5 cm) in the form of the function $\lambda(t)$, are shown by curve 2. The beginning of the slot formation in the computation and the tests agreed with high accuracy and corresponds to the value $t_k \approx 20$ msec.

The authors are grateful to S. S. Grigoryan for attention to the research and for discussion.

LITERATURE CITED

1. H. Kolsky and D. Rider, "Stress and fracture waves," in: Fracture [Russian translation], Vol. 1, Mir, Moscow (1973).
2. G. G. Konstantinov, L. L. Marchenko, and K. N. Shkhinek, "On wave propagation in a bounded elastoplastic rod under longitudinal impact," Fiz. Goreniya Vzryva, No. 4 (1965).
3. J. Mainchen and S. Sak, Computation method 'Tensor,'" in: Calculation Methods in Hydrodynamics [Russian translation], Mir, Moscow (1967).
4. M. N. Gol'dshein, Mechanical Properties of Soils [in Russian], Stroiizdat, Moscow (1971).
5. J. Von Neumann and R. D. Richtmyer, "A method for the numerical calculation of hydrodynamical shocks," J. Appl. Phys., 21, 232 (1950).
6. V. A. Kotlyarevskii and A. G. Chistov, "Numerical analysis of wave diffraction in viscoelastic media under plane strain," Izv. Akad. Nauk SSSR, Mekh. Tverd. Tela, No. 3 (1976).

A POINT EXPLOSION IN A COMPRESSED MULTICOMPONENT MIXTURE

A. M. Maslennikov and V. S. Fetisov

UDC 534.222

Among the various approaches to the study of the motions of a compressed medium, a special place is occupied by self-similar methods for the solution of the hydrodynamic equations, making it possible to reduce the problem to the investigation of ordinary differential equations. In [1] a scheme was developed for the calculation of the self-similar motions of an ideal gas in an incompressible liquid in the case of a strong point explosion; in [2] the methods of [1] were generalized for the case of a strong explosion in a compressible medium. Both pieces of work considered one-component media. At the same time, the study of explosive motions in media consisting of several components is of considerable interest for practical purposes.

In order that the problem of a strong point explosion in a compressible medium be self-similar, it is sufficient that the equation of state of the medium have the form

$$\varepsilon(p, \rho) = \frac{p}{\rho_0} \Phi\left(\frac{\rho}{\rho_0}\right) + \text{const}, \tag{1}$$

where ε is the internal energy; p and ρ are the pressure and the density, respectively; ρ_0 is a constant with the dimensionality of density; and Φ is an arbitrary function of its argument. Directly from relationship (1) there follows the equation of the adiabat of the medium:

$$p(\rho) = \psi(S)\chi(\rho/\rho_0),$$

where S is the entropy. The connection between the functions Φ and χ is determined by the formulas

$$\Phi(R) = \frac{1}{\chi(R)}\left\{c + \int \frac{\chi(R)}{R^2}\, dR\right\}, \quad \chi(R) = \frac{c}{\Phi(R)} \exp \int \frac{dR}{R^2 \Phi(R)}. \tag{1a}$$

Moscow. Translated from Zhurnal Prikladnoi Mekhaniki i Tekhnicheskoi Fiziki, No. 2, pp. 105-109, March-April, 1978. Original article submitted March 11, 1977.

 0021-8944/78/1902-0224$07.50